Supporting Information

On the Chemical Filler-Polymer Interaction of Nano- and Micro-sized ZIF-11 in PBI Mixed Matrix Membranes and their Application for H_2/CO_2 Separation

Javier Sánchez-Laínez, Beatriz Zornoza, Carlos Téllez, Joaquín Coronas*

Chemical and Environmental Engineering Department and Instituto de Nanociencia de Aragón (INA), Universidad de Zaragoza, 50018 Zaragoza, Spain
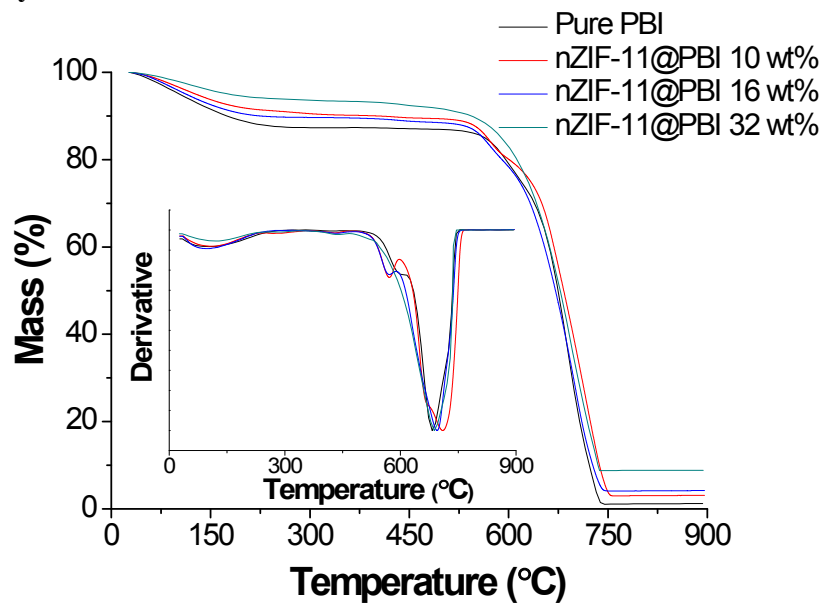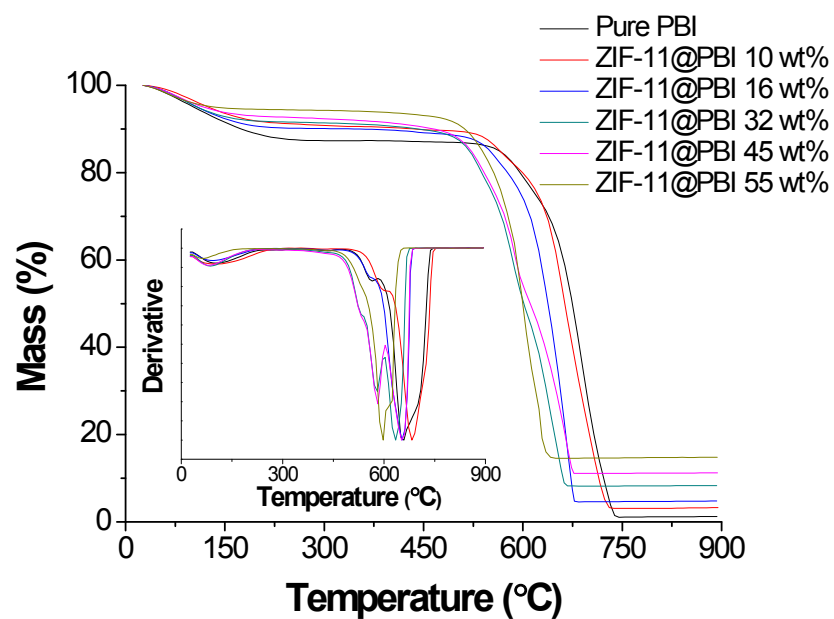
Corresponding author:
Dr. Beatriz Zornoza
Phone: (+34) 876555427; Fax: (+34) 976 761879
E-mail: bzornoza@unizar.es
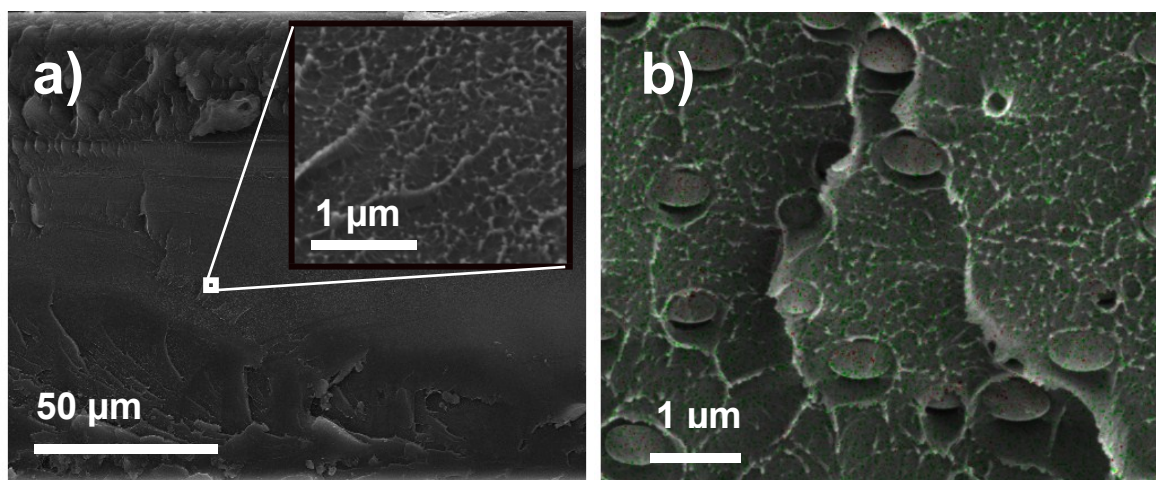
1. TGA analysis:

Figure S1. TGA and derivative curves (inset) of the PBI MMMs prepared with nZIF-11 at several loadings.

Figure S2. TGA and derivative curves (inset) of the PBI MMMs prepared with ZIF-11 at several loadings.

2. EDX mapping:

| EDX (weight %)	C	O	Zn
10 wt% nZIF-11 PBI MMM	84.3	13.0	2.7
16 wt% nZIF-11 PBI MMM	84.2	11.3	4.5

Figure S3. SEM-EDX of the cross-section of a nZIF-11/PBI MMMs at 10 wt% loading (a) and 16 wt% loading (b). EDX-mapping for 16 wt% nZIF-11/PBi MMM is plotted where can be distinguished C (in green) and Zn (in red). Weight % calculated from the whole section in (a) and (b) are included in the table.

3. Stability in DMAc:

In order to know if the morphology changes of both fillers inside the membranes were due to the effect of the solvent at the hard casting conditions, the following experiment was performed. 2 g of ZIF-11 and nZIF-11 were separately dispersed in 2 g of DMAc and the resulting suspension was stirred overnight. The dispersions were three times stirred and sonicated alternately for 90 min total time and cast into a petri dish leveled inside an oven at 90 °C. The petri dishes were left uncovered overnight to allow the evaporation of the solvent. Finally, the resulting powder was characterized by SEM (Fig. S4) and XRD (Fig. S5) analyses.
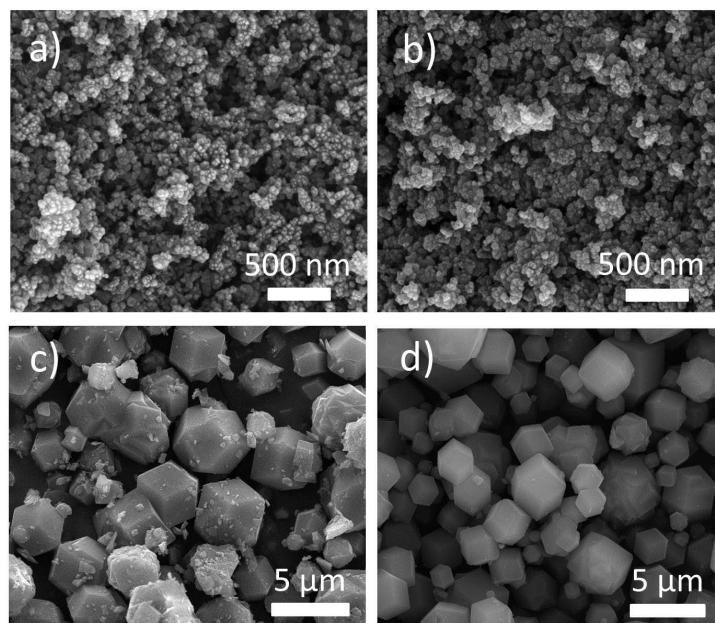
Figure S4. SEM images of nZIF-11 before (a) and after (b) being treated in DMAc and ZIF-11 before (c) and after (d) being treated in the same solvent.
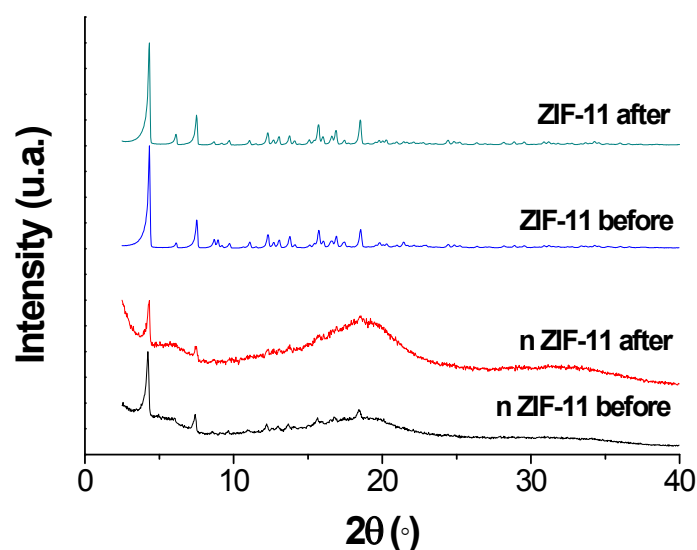
Figure S5. XRD spectra of nZIF-11 before (a) and after (b) being treated in DMAc and ZIF-11 before (c) and after (d) being treated in the same solvent.

As Fig. S4 shows, the morphology of the crystals remain unchanged after having been treated in DMAc. The same happens with their crystallinity, which can be seen from the XRD spectra on Fig S5. Therefore, the morphological changes previously observed in the MMMs images were probably due to the interaction of the filler with the benzimidazole groups of the polymer, which is the same molecule as the organic linker of the ZIFs.

4. Intrinsic properties of the fillers:

In order to get a deeper understanding of the MMMs permeation results, a permeation model was used to estimate the intrinsic properties of the fillers. The chosen model was the Maxwell-Wagner-Sillar equation (Eq. 1) that can calculate the permeability of a MMM (P_{eff}) for the case of a dilute dispersion of ellipsoids:

$$P_{eff} = P_c \cdot \frac{n \cdot P_d + (1 - n)P_c + (1 - n)(P_d - P_c) \cdot \Phi}{n \cdot P_d + (1 - n)P_c - n(P_d - P_c) \cdot \Phi}$$

(Eq. 1)

where n denotes the shape factor of the filler; P_d and P_c, the permeability of the dispersed and continuous phases, respectively; and φ, the fractional volume of the respective phases.

The performance values of the different MMMs at 150 ºC were used to calculate P_d and P_c. For spherical filler particles, thus n = 1/3, the equation reduces to Maxwell equation, which leads to no logical solution in this case of study, since the permeabilities obtained have negative values. Therefore, a parametrization with different shape factor values was performed. The aim was finding matches in the solutions among the different loadings that could elucidate the intrinsic properties of the ZIFs. All those calculated values can be seen in tables S1 and S2, except for the loadings of 10 wt% and 32 wt% for nZIF-11 and ZIF-11, respectively, which resulted in no logical result for each n value.

As it is shown in table S2, there is a tendency in the n value for ZIF-11 MMMs since it tends to decrease as the membrane loading increases. This result is coherent, because the filler augments its aspect ratio (see Fig. 2). On the other hand, there is not such a big difference for nZIF-11 MMMs (Table S2) because the form of the ellipsoids at 16 and 32 wt% loading is more similar between each other (see Fig. 1) Besides, both the permeabilities and the H_2/CO_2 selectivity of ZIF-11 is higher than those of nZIF-11, which can explain the better performance result obtained with the membranes containing the former.

Table S1. Calculated intrinsic properties of nZIF-11 at different membrane loadings together with the average values.

nZIF-11 loading	n value	H_2 permeability (Barrer)	CO_2 permeability (Barrer)	H_2/CO_2 Selectivity (-)
10 wt%	-	-	-	-
16 wt%	0.20	4935	77	64
32 wt%	0.31	4061	64	63
Average	**-**	**4498**	**70**	**64**

Table S2. Calculated intrinsic properties of nZIF-11 at different membrane loadings together with the average values.

ZIF-11 loading	n value	H_2 permeability (Barrer)	CO_2 permeability (Barrer)	H_2/CO_2 Selectivity (-)
10 wt%	0.29	8459	26	325
16 wt%	0.18	8801	72	122
32 wt%	-	-	-	-
45 wt%	0.13	8601	75	114
55 wt%	0.08	10449	176	59
Average	**-**	**9078**	**87**	**104**